

Precision therapy for a new disorder of AMPA receptor recycling due to mutations in *ATAD1*

OPEN 

Rebecca C. Ahrens-Nicklas, MD, PhD*
George K.E. Umanah, PhD*
Neal Sondheimer, MD, PhD
Matthew A. Deardorff, MD, PhD
Alisha B. Wilkens, MS
Laura K. Conlin, PhD
Avni B. Santani, PhD
Addie Nesbitt, PhD
Jane Juulsola, PhD
Erica Ma
Ted M. Dawson, PhD
Valina L. Dawson, PhD
Eric D. Marsh, MD, PhD

Correspondence to Dr. Marsh: marsh@chop.edu

ABSTRACT

Objective: *ATAD1* encodes Thorase, a mediator of α -amino-3-hydroxy-5-methylisoxazole-4-propionate (AMPA) receptor recycling; in this work, we characterized the phenotype resulting from *ATAD1* mutations and developed a targeted therapy in both mice and humans.

Methods: Using exome sequencing, we identified a novel *ATAD1* mutation (p.E276X) as the etiology of a devastating neurologic disorder characterized by hypertonia, seizures, and death in a consanguineous family. We postulated that pathogenesis was a result of excessive AMPA receptor activity and designed a targeted therapeutic approach using perampanel, an AMPA-receptor antagonist.

Results: Perampanel therapy in *ATAD1* knockout mice reversed behavioral defects, normalized brain MRI abnormalities, prevented seizures, and prolonged survival. The *ATAD1* patients treated with perampanel showed improvement in hypertonicity and resolution of seizures.

Conclusions: This work demonstrates that identification of novel monogenic neurologic disorders and observation of response to targeted therapeutics can provide important insights into human nervous system functioning. *Neurol Genet* 2017;3:e130; doi: 10.1212/NXG.000000000000130

GLOSSARY

AMPA = α -amino-3-hydroxy-5-methylisoxazole-4-propionate; **AMPA** = AMPA receptor; **ANOVA** = analysis of variance; **FDA** = Food and Drug Administration; **GABA** = γ -aminobutyric acid; **LOD** = logarithm of the odds; **ROH** = region of homozygosity; **SNP** = single nucleotide polymorphism.

Clinical exome sequencing is becoming a standard of care for patients who remain undiagnosed after extensive diagnostic workup. Although exome sequencing reveals a diagnosis in 25%–40% of patients,^{1–3} obstacles continue to prevent genomic medicine from wide-spread use. Challenges include understanding the effect of gene variants on disease^{4,5} and using genomic information to improve an individual's management.

We report an example of how these challenges can be overcome and, concurrently, describe a monogenic disorder caused by recessive loss-of-function *ATAD1* mutations. Affected neonates demonstrate progressive extreme hypertonia, encephalopathy, and seizures. *ATAD1* encodes Thorase, an AAA+ ATPase that internalizes postsynaptic α -amino-3-hydroxy-5-methylisoxazole-4-propionate receptors (AMPA). AMPAR bind the major excitatory neurotransmitter, glutamate. Activity-dependent insertion and removal of postsynaptic AMPAR are integral to learning and memory.⁶ In *ATAD1* knockout mice,⁷ loss of Thorase decreases internalization of AMPAR, resulting in increased postsynaptic

Supplemental data
at Neurology.org/ng

*These authors contributed equally to this work.

From the Section of Biochemical Genetics (R.C.A.-N., N.S.), Division of Human Genetics (R.C.A.-N., M.A.D., A.B.W.), Department of Pathology and Laboratory Medicine (L.K.C., A.B.S., A.N.), Division of Child Neurology (E.D.M.), Children's Hospital of Philadelphia, PA; Department of Pediatrics (R.C.A.-N., N.S., M.A.D., E.D.M.) and Department of Neurology (E.D.M.), Perelman School of Medicine, and Department of Clinical Pathology (L.K.C., A.B.S.), University of Pennsylvania, Philadelphia; GeneDx (J.J.), Gaithersburg, MD; Neuroregeneration and Stem Cell Programs (G.K.E.U., T.M.D., V.L.D.), Institute for Cell Engineering; Departments of Neurology (G.K.E.U., T.M.D.), Solomon H. Snyder Department of Neuroscience (T.M.D., V.L.D.), Pharmacology and Molecular Sciences (T.M.D., V.L.D.), Physiology (V.L.D.), and Public Health (E.M.), Johns Hopkins University, Baltimore, MD.

Funding information and disclosures are provided at the end of the article. Go to Neurology.org/ng for full disclosure forms. The Article Processing Charge was paid by the authors.

This is an open access article distributed under the terms of the Creative Commons Attribution-NonCommercial-NoDerivatives License 4.0 (CC BY-NC-ND), which permits downloading and sharing the work provided it is properly cited. The work cannot be changed in any way or used commercially without permission from the journal.

receptor density, excitatory neurotransmission, excitotoxicity, and neuronal death. *ATAD1* knockout mice have seizures and die between postnatal days 19 and 25. Given the similarity between mice and humans lacking functional Thorase, we designed a targeted therapeutic approach using the AMPAR antagonist, perampanel,^{8,9} and found that it improves behavior and survival in mice and eliminates seizures and improves tone in patients.

METHODS Further information can be found in the supplemental methods at Neurology.org/ng.

Study design. The objective of this study was to first identify the etiology of the subjects' hypertonia and seizure disorder using exome sequencing and autozygosity mapping. Once the *ATAD1* mutation was identified, the next objective was to evaluate the efficacy of the AMPA receptor antagonist, perampanel, in both a mouse model of *ATAD1*-associated disease and human *ATAD1* patients. For mouse behavioral and imaging studies, a group size of 6 was chosen so that given an SD of 10%, an 18% difference in the mean values between the 2 groups could be detected with a power of 80%. The sample size for the human studies was determined by the number of available patients and family members. The human therapeutic trial was an open-label single-center compassionate use trial in the 2 affected patients. Because of technical limitations, the study was not randomized or blinded. Clinical improvement in the patients was measured using the Functional Status Score, a validated pediatric outcome measurement,¹⁰ see supplemental methods for more details.

Standard protocol approvals, registrations, and patient consents. Animal experiments were performed in compliance with the regulations of the Animal Ethical Committee of the Johns Hopkins University Animal Use and Care Committee. For human studies, written informed consent was obtained for

the trial and for publications of photos and videos. The study was approved by the Children's Hospital of Philadelphia Institutional Review Board. The use of perampanel was approved through a Food and Drug Administration (FDA) emergency investigational new drug application.

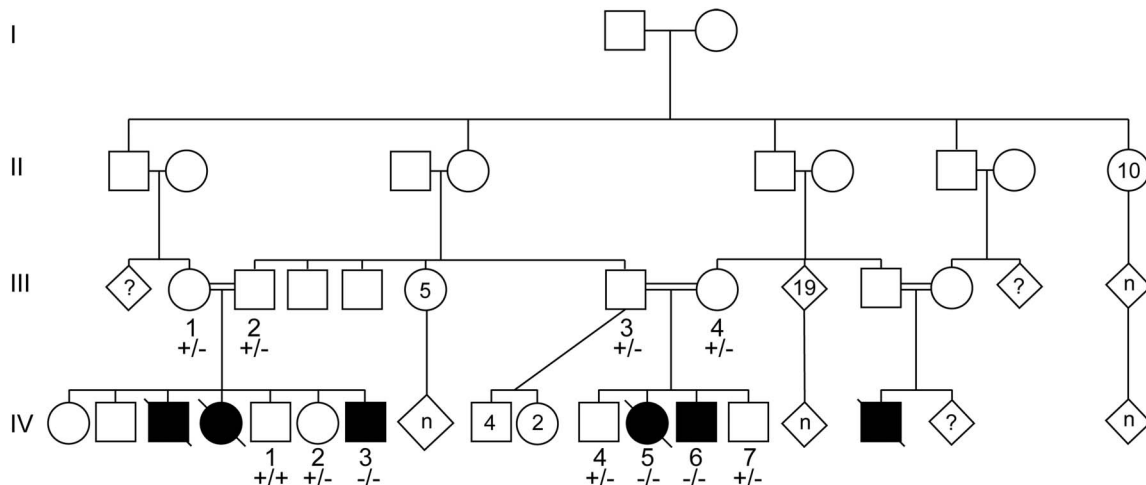
Statistics. Mouse imaging and behavioral data are graphed as mean \pm SD. For statistical analysis of MRI results, distance calculations, and rest measurements, one-way analysis of variance (ANOVA) was performed followed by a Tukey post hoc test to compare mean values. For open-field analysis, a 2-way ANOVA followed by a Sidak post hoc analysis was performed. Multiplicity-adjusted *p* values were calculated. For survival analysis, a log-rank (Mantel-Cox) test was performed.

RESULTS Identification of recessive loss-of-function

***ATAD1* mutations.** To obtain a diagnosis in a large consanguineous Kuwaiti family with multiple neonates affected with hypertonia, seizures, respiratory failure, and death (figure 1, supplemental results), we used clinical exome sequencing and single nucleotide polymorphism (SNP)-based homozygosity analysis. The proband (individual IV-6, figure 1) was symptomatic at birth and presented to our center at age 9 months. He was nonresponsive to tactile, visual, and auditory stimuli with no spontaneous movement and extreme hypertonia. EEG at 9 months showed hypersarrhythmia, a chaotic interictal pattern suggestive of severe brain dysfunction. He did not demonstrate infantile spasms as his extreme hypertonia precluded almost all movement. Brain MRI at 2 months of life was normal, but repeat at 9 months showed marked interval reduction in cerebral volume. Prior investigations (table 1) were unrevealing.

The second patient was the proband's 2-month old male cousin (individual IV-3, figure 1). He also

Figure 1 Subjects' pedigree demonstrates multiple affected individuals in a highly consanguineous family



The proband is patient IV-6; his cousin who was subsequently evaluated and treated is patient IV-3. The *ATAD1* variant, p.E276X, was identified by whole-exome sequencing and tracked with disease in all available family members (+ represents the normal allele and - represents the p.E276X allele). See also figure e-1.

Table 1 Initial examination features and prior evaluations for patient IV-6 and patient IV-3

	Patient IV-6	Patient IV-3
Initial phenotypic features		
Age at initial evaluation, mo	9	2.5
Age at symptom onset	Birth	Birth
Age at initiation of perampanel, mo	16	2.5
Age at first intubation, mo	1	3.5
Dysmorphic facial features	No	No
Birth growth percentiles	50th-75th	Small for gestational age
Hypertonia	Yes	Yes
Clinical seizures outside hospital	Yes	Yes
Reactive pupils on examination	No	Yes
Present gag reflex	No	Yes
Able to blink to threat	No	No
Able to withdraw from pain	No	Yes
Hyperreflexia	Yes	No
Inguinal hernia	Yes	Yes
Scoliosis	Yes	Yes
Diagnostic evaluations		
Brain MRI at 2 mo	Normal	Normal
Repeat MRI (age in months)	Progressive volume loss (9, 20)	Normal (5)
Brain MR spectroscopy	Normal	Normal
EEG	Hypsarrhythmia	Abnormal background
Cardiac echocardiogram	Normal	Normal
Renal ultrasound	Multicystic dysplastic left kidney	Normal
Muscle biopsy	Normal	Not done
Serum lactate	Normal	Normal
Serum CK	Normal	Normal
Urine organic acids	Normal	Normal
Plasma amino acids	Normal	Normal
Plasma acylcarnitine profile	Normal	Not done
Alanine aminotransferase, U/L (normal 5-45 U/L)	47	44
Aspartate aminotransferase, U/L (normal 20-60 U/L)	102	62
Karyotype	46, XY	46, XY
Early infantile epilepsy gene panel	No mutation	Not done

Abbreviations: CK = creatine kinase; MR = magnetic resonance.

had a history of hypertonia and clinical seizures at birth. On first evaluation at our center at 2.5 months of age, he had little spontaneous movement and was extremely stiff (video 1). EEG at presentation while on phenobarbital demonstrated a background lacking normal mixture of frequencies and poorly formed sharps but no seizures. Brain MRI was unremarkable.

Exome sequencing of patient IV-6 revealed no mutations in known disease-causing genes. However,

a homozygous nonsense variant of unknown significance in *ATAD1* (c.826 G>T, p.E276X) was reported (figure e-1A). His parents each carried 1 copy of the change. The variant was classified as having a potential relationship to a disease phenotype. There are no previous reports of *ATAD1* mutations in humans; however, mice harboring mutations in *ATAD1* have frequent seizures, hypertonia, and early death.⁷ Compound heterozygote variants of unknown significance were also found in *SZT2*, which causes autosomal recessive epileptic encephalopathy type 18; however, the variants did not segregate in his affected sister (IV-5) and he did not fit this phenotype (supplemental results).

SNP analysis confirmed that the family was consanguineous (table e-1). Patient IV-6 was found to have a de novo 1.25 Mb duplication of 17p13.3 (for more details, see supplemental results). Overlapping duplications have been reported with variable phenotypes including mild dysmorphic features, learning disability, hypotonia, autism spectrum disorder, and mild brain abnormalities.¹¹ This duplication was not present in affected individuals IV-3 or IV-5. Furthermore, given the extreme hypertonia and early respiratory failure seen in individual IV-6, we did not feel that this could fully explain his phenotype.

Homozygosity mapping revealed that the patient (IV-6), his deceased affected sister (IV-5), and affected cousin (IV-3) shared only one region of homozygosity (ROH) that was not shared with any unaffected relative (III 1-4 and IV-1, 2, and 7). This 6.5 Mb shared ROH (chr10:83,619,940-90,095,915, hg19 coordinates) contained 28 protein-coding genes, 14 of which are associated with a known disease phenotype (tables e-2 and e-3). *ATAD1* is located in this shared ROH, while *SZT2*, the other candidate gene identified through exome sequencing, is not. Molecular analysis confirmed that all affected family members were homozygous for the p.E276X variant, while unaffected family members were not (figure 1). Multipoint genetic linkage analysis of 8 SNPs as markers in this region demonstrated a logarithm of the odds (LOD) score of 3.7 (table e-4), while the LOD score calculated directly using only the *ATAD1* p.E276X variant was 3.5. An LOD score ≥ 3.3 has been shown to correspond to a genome-wide significance level of <0.05 .¹²

The effect of the p.E276X variant on *ATAD1* expression was investigated in lymphoblastoid cells derived from the patient and an unaffected control. *ATAD1* messenger RNA expression was decreased by 78% in p.E276X cells. This degree of reduction is consistent with nonsense-mediated decay,¹³ as noted by the absence of Thorase protein on Western blotting (figure e-1B). Investigation of *ATAD1* variation in control populations revealed that in the Exome

Aggregation Consortium (exac.broadinstitute.org/gene/ENSG00000138138) database, only 3 loss-of-function variants were observed in the gene, while the expected number of loss-of-function variants is 14.9. This suggests selection against loss-of-function mutations in *ATAD1*.

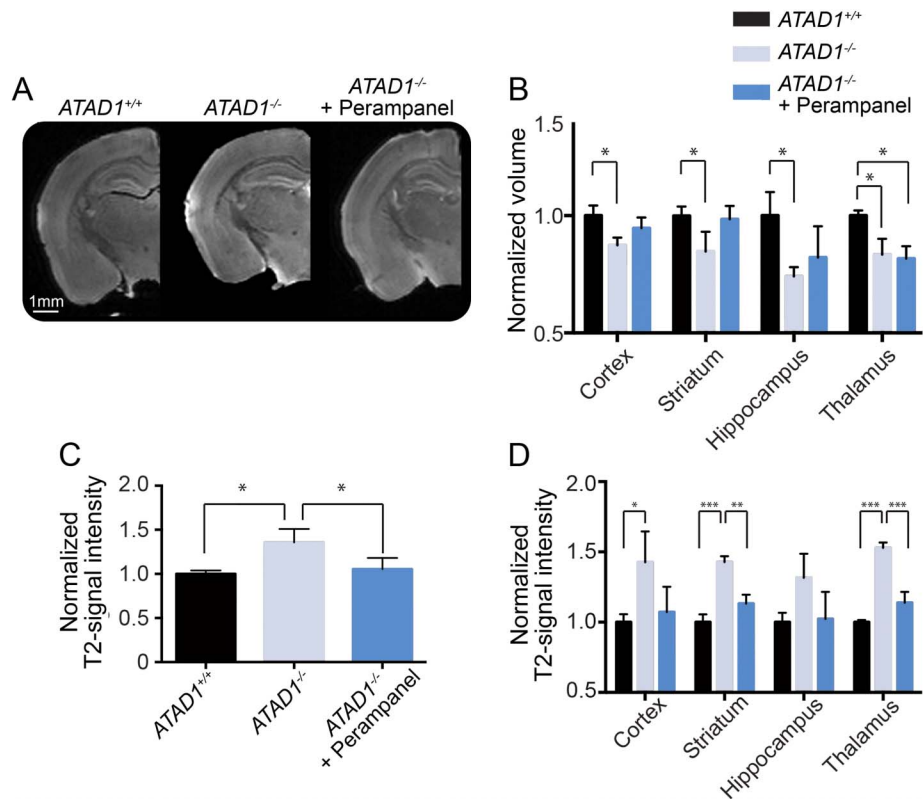
Evaluation of perampanel as a therapeutic approach. Given that the p.E276X variant tracked with disease, decreased *ATAD1* expression, and that *ATAD1* knockout mice died of seizures, we concluded that this mutation was likely pathogenic. *ATAD1* mutations increase AMPA receptor-mediated excitatory signaling due to impaired receptor recycling.⁷ Considering this mechanism of disease, we hypothesized that perampanel,^{14,15} a noncompetitive AMPAR antagonist could have therapeutic benefit. Therefore, we investigated the efficacy of perampanel in *ATAD1*^{-/-} mice. Perampanel dosing in mice was based on prior studies⁸ and a dose escalation study (figure e-2).

Perampanel response in mice. Ex vivo brain MRI of *ATAD1*^{-/-} mice (figure 2A) demonstrated a volume

reduction in all areas examined as compared to controls. Perampanel treatment did not show significant prevention of volume loss; however, there was a trend toward improvement (figure 2B). Loss of *ATAD1* was also associated with increased T2-signal intensity throughout the brain, which is indicative of brain pathology with increased fluid content (figure 2C). Perampanel improved whole-slice signal intensity in *ATAD1*^{-/-} animals by 30.3% (95% confidence interval 11.3%–59.5%); further analysis of individual brain regions revealed improvement of signal intensity in the thalamus and striatum (figure 2D).

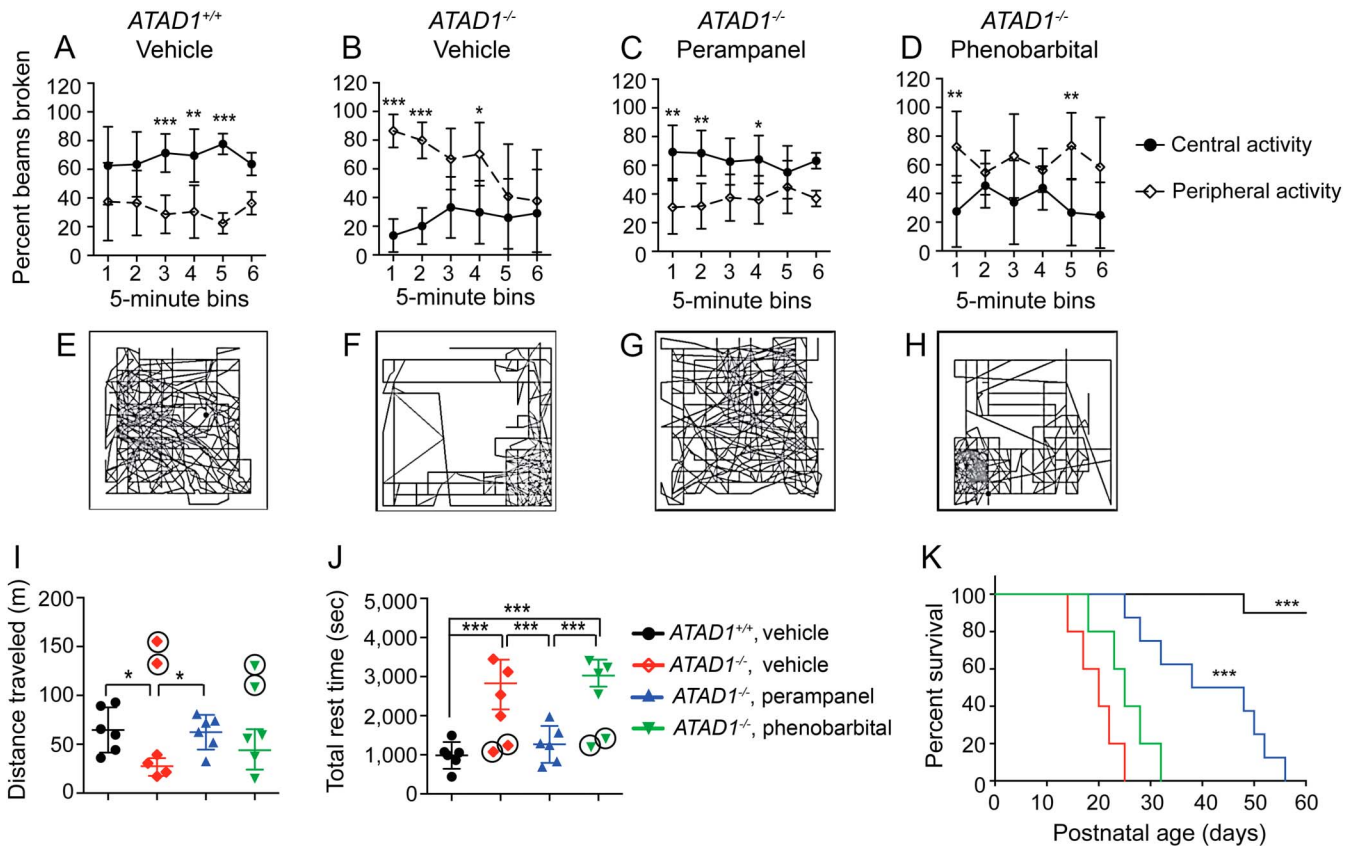
On open-field activity testing, *ATAD1*^{-/-} mice showed both an abnormal activity pattern as compared to wild-type mice (figure 3, A–H) and decreased spontaneous movements as measured by the distance traveled and the total rest time (figure 3, I and J). Perampanel corrected these behavioral deficits, while phenobarbital, an antiepileptic that targets γ -aminobutyric acid (GABA) receptors rather than AMPA receptors, did not. *ATAD1*^{-/-} mice

Figure 2 Perampanel improves brain MRI differences in *ATAD1*^{-/-} mice



(A) Representative ex vivo brain MRIs of wild-type and *ATAD1*^{-/-} perampanel-treated and perampanel-untreated mice. (B) Untreated *ATAD1*^{-/-} mice (light blue bars) demonstrated volume reduction in all brain areas measured as compared to *ATAD1*^{+/+} mice (black bars). Perampanel therapy (dark blue bars) was associated with a trend toward normalization of brain volumes. (C) Whole-slice T2 MRI signal intensity was significantly increased in *ATAD1*^{-/-} mice. This change was reversed with perampanel therapy. (D) T2-signal intensity was increased in *ATAD1*^{-/-} mice throughout the brain. Perampanel therapy normalized signal intensity in the striatum and thalamus. For all panels, n = 6. *p = 0.01–0.05, **p = 0.001–0.009, and ***p < 0.001.

Figure 3 Perampanel normalizes behavior and prolongs survival in *ATAD1*^{-/-} mice



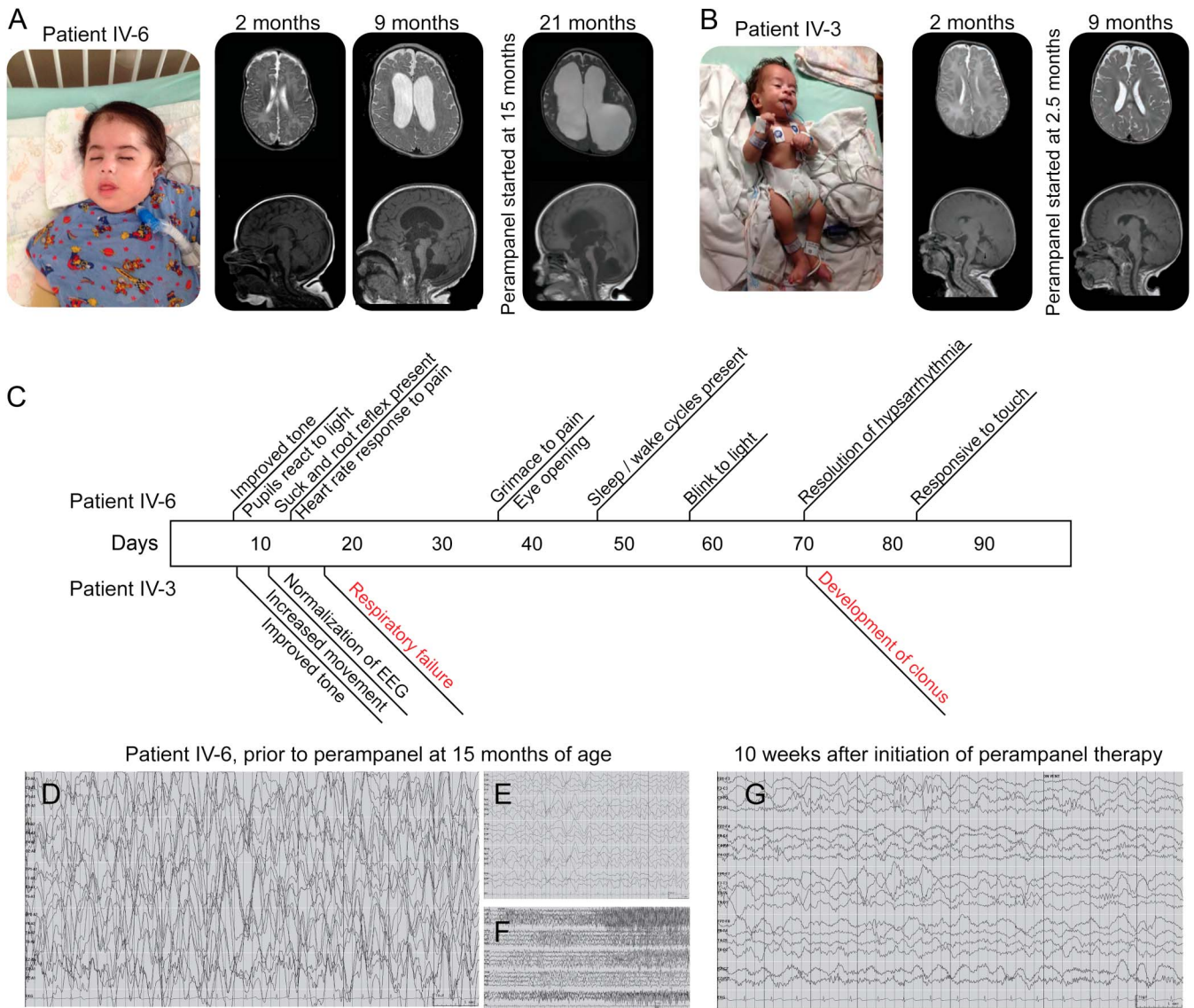
(A–H) Perampanel, but not phenobarbital, normalized open-field assessments in *ATAD1*^{-/-} mice as seen by quantification (A–D) and representative pathview images (E–H) from (A, E) vehicle-treated, *ATAD1*^{+/+}, (B, F) vehicle-treated, *ATAD1*^{-/-}, (C, G) perampanel-treated, *ATAD1*^{-/-}, and (D, H) phenobarbital-treated, *ATAD1*^{-/-} mice (n = 6). Open circles represent peripheral activity; closed circles represent central activity. (I and J) On behavioral analysis, *ATAD1*^{-/-} mice (red diamonds) cover less distance (L) and rest more (M) than their wild-type littermates (black filled-in circles). Perampanel (blue triangles) reverses the movement deficits, while phenobarbital does not (n = 6). Two mice in the *ATAD1*^{-/-} perampanel and phenobarbital-treated groups seized during this observation. The seizures were characterized by high-speed involuntary movements; therefore, they are shown in the figure (symbol surrounded by a black circle), but they are not included in the statistical analysis. (K) Survival is prolonged from 20 days in vehicle-treated *ATAD1*^{-/-} mice (red line) to 43 days in *ATAD1*^{-/-} perampanel-treated mice (blue line). There is no statistical survival difference between *ATAD1*^{-/-} mice treated with vehicle (red line) or phenobarbital (green line). For all panels, *p = 0.01–0.05, **p = 0.001–0.009, and ***p < 0.001. See also figures e-2 and e-3.

showed no difference in rearing activity or average speed as compared to wild-type littermates (figure e-3). Extensive daily observations revealed that *ATAD1*^{-/-} mice would have seizures on the day that they died. Video recording revealed that 5 of 5 vehicle-treated, as compared to zero of 5 perampanel-treated, *ATAD1*^{-/-} mice demonstrated seizures (video 2). Finally, perampanel significantly prolonged average survival in *ATAD1*^{-/-} mice by 115% (mean of 20 vs 43 days), while phenobarbital did not significantly increase survival (figure 3K). These results demonstrate the efficacy of targeted AMPAR blockade by perampanel in mice with impaired AMPAR endocytosis due to mutations in *ATAD1*.

Perampanel response in humans. Given the efficacy of perampanel in mice, we next considered a therapeutic trial in patients with *ATAD1* mutations. Perampanel was recently approved by the FDA for the treatment of seizures and demonstrated minimal

off-target toxicity in human studies¹⁵; we obtained permission for off-label compassionate use for treatment of affected individuals. Patient IV-6 was started on perampanel at 16 months of age; at this time, he had severe brain atrophy on MRI (figure 4A), hypertonia, absent cranial nerve reflexes, no spontaneous respiratory drive, and hypersarrhythmia on EEG. Within 8 days of starting perampanel, his tone improved and he developed a pupillary response to light. He continued to show dose-dependent neurologic improvement until his neurologic status plateaued at a dose of approximately 0.5 mg/kg/d (figures 4C, e-4, e-5). He also had resolution of hypersarrhythmia on EEG (figure 4, D–G). He was weaned off all nonperampanel antiepileptics, which included phenobarbital (dose at start of trial 6 mg/kg/d), topiramate (dose at start of trial 6 mg/kg/d), and valium (dose at start of trial 0.9 mg/kg/d). Despite therapy, he continued to have severe neurologic

Figure 4 Perampanel improves hypertonicity, prevents seizures, and slows neurodegeneration but cannot normalize neurologic function in patients with *ATAD1* mutations



(A) Photographs and brain MRIs of the proband, individual IV-6. Initial brain MRI at 2 months showed normal parenchyma, but subsequent studies at 9 and 21 months showed progressive volume loss and hydrocephalus. (B) Photographs and brain MRI of patient IV-3. Brain MRI at 2 months of age was normal. Perampanel was started at 2.5 months of age and follow-up MRI at 9 months of age showed no changes (unlike the progressive neurodegeneration seen in untreated patient IV-6 over the same age range, panel A). (C) Timeline of clinical improvements observed in patient IV-6 and patient IV-4 after the initiation of perampanel therapy. Patient IV-4 also had progression of disease (marked in red) including respiratory failure that was not prevented with perampanel. The bottom panel shows an EEG recorded from subject IV-6 at 15 months of age, prior to therapy with perampanel. (D) Hypsarrhythmia is seen on EEG (gain = 7 $\mu\text{V}/\text{mm}$). (E) The pretreatment recording from panel A is shown at a gain of 30 $\mu\text{V}/\text{mm}$. (F) An example of one of many focal seizures captured on routine EEG prior to perampanel. The lower panel shows the EEG of the same patient 10 weeks after starting perampanel. (G) While on perampanel, the hypersarhythmia resolved and no focal seizures were noted on follow-up 60-minute routine EEG. This improved EEG pattern was noted on all subsequent follow-up EEGs recorded over a several month period of observation. See also figure e-4.

deficits and worsening hydrocephalus requiring endoscopic third ventriculostomy.

In light of the clinical improvement seen in the proband, patient IV-3 was started on perampanel at 2.5 months of age. Given his young age, his neurologic function was more intact as compared to his cousin's at the start of therapy. While he was profoundly hypertonic, he had normal cranial nerve reflexes and respiratory drive. After starting

perampanel, he had rapid improvement in tone and normalization of his EEG (video 1). Like his cousin, he was weaned from his other seizure medications including phenobarbital (dose at start of trial of 2.5 mg/kg/d). Repeat brain MRI at 9 months of age showed no parenchymal volume loss while on perampanel (figure 4B), a finding that is dramatically different from what was seen in the proband at age 9 months (figure 4A, middle MRIs). Despite these

markers of improvement, he developed respiratory failure requiring intubation. However, his limited function was better as compared to his cousin who was untreated at the same age: he maintained all brain stem reflexes, sleep/wake cycles, the ability to withdraw and vocalize to pain, and spontaneous movements of all extremities (figure 4C, and supplemental information).

Functional improvement was also measured using the functional status score, a validated pediatric outcome measurement.¹⁰ This outcome assesses 6 functional domains (mental status, sensory, communication, motor, feeding, and respiratory function), each on a scale from 1 (normal) to 5 (severely impaired), and a composite score is calculated. Fully functioning children receive a score of 6, while maximal impairment is assigned a score of 30. Over the course of therapy, patient IV-6 had a score improvement from 29 to 24 (figure e-4, A and B). Patient IV-4 began the trial with a functional status score of 19 and showed an initial improvement to a low score of 17. However, his overall functional score worsened despite therapy at 3–4 months of age due to his respiratory failure (figure e-4, C and D). At the end of the therapeutic trial, his functional status score plateaued at 23, as compared to his untreated cousin's score of 29 at the same age. This suggests that perampanel may improve functional outcomes but cannot completely prevent progression of disease.

DISCUSSION We describe a disorder of AMPAR recycling caused by mutations in *ATAD1*, a gene not previously known to cause human disease. Affected patients demonstrate hypertonicity, seizures, and early death. Targeted therapy with perampanel alters the pathogenic mechanism and provides benefit in both mouse models and patients.

This case series demonstrates the power of combining genomic testing and variant analysis using animal models. In addition, we confirm that combining detection of variants in novel genes and an understanding of disease mechanisms can inform care of an individual. This effort has achieved a clinical diagnosis, improved understanding of AMPAR function, and suggested therapeutic options.

As the first report of *ATAD1*-induced human disease, this work builds on previous observations that mutations that interrupt normal synaptic transmission can cause seizures.^{16,17} Postsynaptic receptor recycling is a known pathogenic mechanism in epilepsy; for example, mutations in *KIF5A* reduce postsynaptic expression of inhibitory GABA_A receptors, reducing total inhibition and leading to seizures and encephalopathy.¹⁸ Unlike *KIF5A* mutations that decrease total inhibition, *ATAD1* mutations increase the

population of excitatory postsynaptic receptors. Ultimately, either mechanism can disrupt the delicate balance between inhibitory and excitatory signaling and induce seizures.

While this study highlights the promise of personalized medicine, there are limitations to this work. *ATAD1* mutations have been identified in only one family. Typically, a gene is not considered as disease causing until it has been observed in 2 families. In this case, we have accumulated multiple lines of evidence supporting the pathogenicity of *ATAD1*. First, the variant tracked within the family and LOD scores calculated both by a multipoint analysis method and the *ATAD1* variant itself showed statistically significant linkage. Second, we functionally showed loss of *ATAD1* protein in patient lymphocytes. Third, it is a stop-gain mutation and is absent from multiple control populations, and multiple computation programs predict its pathogenicity. Lastly, the *ATAD1* p.E276X variant is classified as pathogenic when applying the recently published ACMG variant analysis guidelines criteria for classification.⁵

As this is a new, ultra-rare disorder, there is limited understanding of its natural history. This makes evaluation of perampanel efficacy difficult. For example, patient IV-3 required tracheostomy despite treatment with perampanel. It is possible that therapy was initiated too late in the natural progression of the disease or at too low of a dose to prevent this outcome. Nonetheless, he had better preservation of neurologic function than the few known untreated family members at the same age. The superior functional status scores in our patient initiated at a younger age could be related to drug effect or due to interindividual variation. Furthermore, we used an open-label therapeutic intervention strategy. This raises the possibility that treating physicians could be biased as to effect. To offset this, we used independent evaluation by multiple physicians. Clearly, more work is needed to fully determine the efficacy of perampanel in this syndrome and to elucidate the exact treatment paradigm to maximize outcomes.

Recently, a second function of *ATAD1* was reported; it acts as part of a quality control system for the mitochondrial membrane.¹⁹ It is unclear how this function may relate to the patients' phenotype; perampanel would not be expected to reverse deficits in this pathway.

Despite the clear benefits of this individualized medicine approach, there is likely an intrinsic limitation to the maximal benefit of perampanel therapy in patients with *ATAD1* mutations. The high doses required in this disorder also inhibit the more subtle modulation of AMPA receptor activity that is crucial

for normal CNS functioning. This limitation is supported by the fact that although perampanel prolongs survival and stops seizures in *ATAD1*^{-/-} mice, they still die at a younger age as compared to their wild-type littermates.

Mice and humans with mutations in *ATAD1*, a mediator of AMPA receptor recycling, manifest with a devastating neurologic disorder that responds to targeted therapy with an FDA-approved AMPA-receptor blocker, perampanel. These first studies establish the promise of this approach, but further studies are needed to elucidate both the natural history and the therapeutic potential of perampanel in patients with *ATAD1* mutations.

AUTHOR CONTRIBUTIONS

Designing research studies: R.C.A.-N., G.K.E.U., N.S., M.A.D., T.M.D., V.L.D., and E.D.M. Statistical analysis: R.C.A.-N. and G.K.E.U. Conducting experiments: R.C.A.-N., G.K.E.U., N.S., M.A.D., A.B.W., L.K.C., A.B.S., A.N., J.J., E.M., and E.D.M. Analyzing data: R.C.A.-N., G.K.E.U., N.S., M.A.D., A.B.W., L.K.C., A.B.S., A.N., J.J., E.M., T.M.D., V.L.D., and E.D.M. Writing the manuscript: R.C.A.-N. and G.K.E.U. Editing the manuscript: R.C.A.-N., G.K.E.U., N.S., M.A.D., L.K.C., J.J., T.M.D., V.L.D., and E.D.M.

STUDY FUNDING

This work was supported by the NIH/NIDA DA000266 and NIH/National Institute of Neurological Disorders and Stroke R01 NS067525 and R37 NS067525 to T.M.D. and V.L.D., and NIH/National Institute of Neurological Disorders and Stroke R01 NS082761-01A1 to E.D.M.

DISCLOSURE

Dr. Ahrens-Nicklas has received research support from NIH. Dr. Umanah reports no disclosures. Dr. Sondheimer was an expert witness on behalf of Par Pharmaceuticals in litigation unrelated to this article. Dr. Deardorff and Ms. Wilkens report no disclosures. Dr. Conlin has served on the scientific advisory board of NIGMS Human Genetic Cell Repository SAC; has received speaker honoraria from Arcadia University; and has received research support from NIH/NHGRI and the Children's Hospital of Philadelphia. Dr. Santani has received speaker honoraria from Agilent; receives publishing royalties from Clinical Research Exome Agilent; has been a consultant for Invitae; has served on the speakers' bureaus of CHI, Biomarker, and World Diagnostics; has received research support from NIH; and has received royalty payments from Agilent. Dr. Nesbitt reports no disclosures. Dr. Juusola has been an employee of GeneDx. Ms. Ma reports no disclosures. Dr. Dawson has served on the scientific advisory board of CurePSP, the Bachmann-Strauss Dystonia and Parkinson Foundation, the Michael J. Fox Foundation for Parkinson's Research, the Milken Institute Parkinson's Disease Scientific Advisory Group Accelerating Medicines Partnership (AMP), the Foundation for the NIH, Technical Working Group Scientific Program Executive Committee, and International Association of Parkinsonism and Related Disorders (IAPRD); has received a speaker honorarium for "Molecular Underpinnings of Parkinson's Disease: A New Path for Therapies"; has served on the editorial boards of *Biology and Chemistry of Nitric Oxide*, the *International Journal of Molecular Medicine*, *Molecular Neurodegeneration*, *Proceedings of the National Academy of Sciences, USA 2007*, *Current Chemical Biology*, *The Open Neuroscience Journal*, *ASN Neuro*, the *American Journal of Clinical Neurology*, *Cell*, the *Journal of Clinical Investigation*, *Parkinson's Disease*, *PLoS One*, the *Journal of Parkinson's Disease*, the *American Journal of Neurodegenerative Disease*, *Synapse*, *F1000 Research*, *Molecular & Cellular Oncology*, *Scientific Reports*, and *Oncotarget*; holds the following patents: #S5266594—Inhibition of nitric oxide synthase and use thereof to prevent glutamate neurotoxicity; #S5587384—Inhibitors

of poly (ADP-ribose) synthetase and use thereof to treat NMDA neurotoxicity; #5,898,029—Direct influences on nerve growth of agents that interact with immunophilins; #S5798355—Inhibitors of rotamase enzyme activity; #S5843960—Inhibitors of rotamase enzyme activity; #S5846981—Inhibitors of rotamase enzyme activity; #SRE036397—Inhibitors of poly (ADP-ribose) synthetase and use thereof to treat NMDA neurotoxicity; #6022878—Inhibitors of rotamase enzyme activity; #6,080,753—Stimulating nerve growth with immunophilins; #6,358,975—Method of using selective PARP inhibitors to prevent or treat neurotoxicity; #6,362,160—Immunophilin-binding agents prevent glutamate neurotoxicity associated with vascular stroke and neurodegenerative diseases; #8603994—Transcriptional repression leading to Parkinson's disease; PCT/US10/4487—LRRK2-mediated neuronal toxicity; 13/294,938—Compounds and related methods for manipulating PARP-1-dependent cell death; 13/294,884—The treatment and prevention of pathologic conditions using iduna and—related techniques and compositions; long-acting GLP-1R agonist as a therapy of neurological and neurodegenerative conditions; US 9,274,128 B2—Transcriptional repression leading to Parkinson's disease; and US 9309208B2—Methods of making and using thioxothiazolidine and rhodamine derivatives as HIV-1 and JSP-1 inhibitors; receives publishing royalties from Elsevier and Informa Healthcare USA, Inc.; has been a consultant for Valted LLC, American Gene Technologies International, Dong-A Pharmaceuticals, and SPARC; and has received research support from AbbVie Pharmaceuticals, Dong-A ST Pharmaceuticals, NIH/National Institute of Neurological Disorders and Stroke/NCBI, the JPB Foundation, the Diana Helis Henry Medical Research Foundation, the Adrienne Helis Malvin Medical Research Foundation, and the Michael J. Fox Foundation. Dr. Dawson has served on the scientific advisory boards of the New York Stem Cell Foundation and the Burke Medical Center Advisory Board; has received travel funding from the Salk Institute, the Gordon Research Conference, the University of Rochester, Novartis, Delaware Biotechnology Institute, Georgetown University, and the University of California San Francisco; has served on the editorial boards of the *Journal of Neuroscience*, *NeuroMolecular Medicine*, the *Journal of Parkinson's Disease*, *Molecular & Cellular Oncology*, *Oncotarget*, the *Journal of Molecular Medicine*, *Neurobiology of Disease*, and *Nitric Oxide*; holds the following patents: S5266594—Inhibition of nitric oxide synthase and use thereof to prevent glutamate neurotoxicity; S5587384—Inhibitors of poly (ADP-ribose) synthetase and use thereof to treat NMDA neurotoxicity; SRE036397—Inhibitors of poly (ADP-ribose) synthetase and use thereof to treat NMDA neurotoxicity; 6,358,975—Method of using selective PARP inhibitors to prevent or treat neurotoxicity; 6,362,160—Immunophilin-binding agents prevent glutamate neurotoxicity associated with vascular stroke and neurodegenerative diseases; PCT/US10/55,857—LRRK2-mediated neuronal toxicity; 8603994—Transcriptional repression leading to Parkinson's disease; and U.S. Provisional Application. Long-Acting GLP-1R Agonist as a Therapy Of Neurological and Neurodegenerative Condition; and has received research support from Inhibikase Therapeutics Inc., AbbVie, Sanofi, Dong-A ST, NIH/NIDA, NIH/National Institute of Neurological Disorders and Stroke, the Adrienne Helis Malvin Medical Research Foundation, and the Diana Helis Henry Medical Research Foundation. Dr. Marsh has served on the scientific advisory boards of Stanley Brothers Social Enterprises and the Jefferson University Cannabis Research and Education Center; serves on the editorial board of *Epilepsia*; and has received research support from GW Pharma, Zogenix Pharmaceuticals, Neuren Pharmaceuticals, and NIH. Go to Neurology.org/ng for full disclosure forms.

Received October 11, 2016. Accepted in final form December 13, 2016.

REFERENCES

1. Yang Y, Muzny DM, Reid JG, et al. Clinical whole-exome sequencing for the diagnosis of Mendelian disorders. *N Engl J Med* 2013;369:1502–1511.
2. Srivastava S, Cohen JS, Vernon H, et al. Clinical whole exome sequencing in child neurology practice. *Ann Neurol* 2014;76:473–483.

3. Yang Y, Muzny DM, Xia F, et al. Molecular findings among patients referred for clinical whole-exome sequencing. *JAMA* 2014;312:1870–1879.
4. MacArthur DG, Manolio TA, Dimmock DP, et al. Guidelines for investigating causality of sequence variants in human disease. *Nature* 2014;508:469–476.
5. Richards S, Aziz N, Bale S, et al. Standards and guidelines for the interpretation of sequence variants: a joint consensus recommendation of the American College of Medical Genetics and Genomics and the Association for Molecular Pathology. *Genet Med* 2015;17:405–423.
6. Kessels HW, Malinow R. Synaptic AMPA receptor plasticity and behavior. *Neuron* 2009;61:340–350.
7. Zhang J, Wang Y, Chi Z, et al. The AAA+ ATPase Thorase regulates AMPA receptor-dependent synaptic plasticity and behavior. *Cell* 2011;145:284–299.
8. Hanada T, Hashizume Y, Tokuhara N, et al. Perampanel: a novel, orally active, noncompetitive AMPA-receptor antagonist that reduces seizure activity in rodent models of epilepsy. *Epilepsia* 2011;52:1331–1340.
9. Zwart R, Sher E, Ping X, et al. Perampanel, an antagonist of α -amino-3-hydroxy-5-methyl-4-isoxazolepropionic acid receptors, for the treatment of epilepsy: studies in human epileptic brain and nonepileptic brain and in rodent models. *J Pharmacol Exp Ther* 2014;351:124–133.
10. Pollack MM, Holubkov R, Glass P, et al. Functional Status Scale: new pediatric outcome measure. *Pediatrics* 2009;124:e18–e28.
11. Curry CJ, Rosenfeld JA, Grant E, et al. The duplication 17p13.3 phenotype: analysis of 21 families delineates developmental, behavioral and brain abnormalities, and rare variant phenotypes. *Am J Med Genet A* 2013;161A:1833–1852.
12. Ott J, Wang J, Leal SM. Genetic linkage analysis in the age of whole-genome sequencing. *Nat Rev Genet* 2015;16:275–284.
13. Popp MWL, Maquat LE. Organizing principles of mammalian nonsense-mediated mRNA decay. *Annu Rev Genet* 2013;47:139–165.
14. Rogawski MA. AMPA receptors as a molecular target in epilepsy therapy. *Acta Neurol Scand Suppl* 2013;197:9–18.
15. Rogawski MA, Hanada T. Preclinical pharmacology of perampanel, a selective non-competitive AMPA receptor antagonist. *Acta Neurol Scand Suppl* 2013;197:19–24.
16. Saitsu H, Kato M, Mizuguchi T, et al. De novo mutations in the gene encoding STXBP1 (MUNC18-1) cause early infantile epileptic encephalopathy. *Nat Genet* 2008;40:782–788.
17. Boumil RM, Letts VA, Roberts MC, et al. A missense mutation in a highly conserved alternate exon of dynamin-1 causes epilepsy in fitful mice. *PLoS Genet* 2010;6:e1001046.
18. Nakajima K, Yin X, Takei Y, Seog DH, Homma N, Hirokawa N. Molecular motor KIF5A is essential for GABA(A) receptor transport, and KIF5A deletion causes epilepsy. *Neuron* 2012;76:945–961.
19. Chen YC, Umanah GKE, Dephoure N, et al. Msp1/ATAD1 maintains mitochondrial function by facilitating the degradation of mislocalized tail-anchored proteins. *EMBO J* 2014;33:1548–1564.